Electromagnetic Resonances of Natural Grasslands and Their Effects on Radar Vegetation Index

Shimaa A. M. Soliman[1, *], Khalid F. A. Hussein[1], and Abd-El-Hadi A. Ammar[2]

Abstract—The present paper studies the characteristics of electromagnetic scattering from vegetation models constructed as random wire structures for the purpose of PolSAR imaging and ground surface cover recognition and classification. Radar vegetation index (RVI) has been developed for the purpose of vegetation growth monitoring. A new method is proposed to use the RVI as an accurate monitor for the natural grassland height taking into account the operational parameters such as the PolSAR look angle and the operating frequency. Also, the present paper addresses a problem that may lead to false indications of the RVI measured for grassland areas. It frequently occurs that some of the narrow long leaves of the grass cloud are quasi-parallel and of nearly equal lengths leading to the generation of internally resonant modes. The enhancement or diminishing of the backscattered field at such internal resonances may give false indication of the RVI, and hence, wrong information can be estimated such as the water content and the grass height. A new method is proposed to model the natural grasslands as clouds of electrically conductive random curly strips for the purpose of obtaining the backscatter coefficients and, hence, the corresponding RVI. The error in height estimation using the proposed method due to the existence of the internal resonances is numerically investigated.

1. INTRODUCTION

Earth remote sensing via satellites is an effective way for management of environmental resources such as measuring and monitoring vegetation areas. Compared with spaceborne optical sensors used for earth remote sensing, Polarimetric Synthetic Aperture Radar (PolSAR) allows high spatial resolution imaging and has the ability to penetrate clouds acquire data independently of weather conditions and sunlight illumination it is useful for the observation of dynamic processes on the Earth's surface. At the appropriate microwave frequencies, PolSAR signals can pass through vegetation canopy, allowing observation of the underlying surface [1]. A PolSAR system has been used to monitor biophysical conditions of various crops that include wheat, soybean, corn, alfalfa, cotton, and rice [2–4].

One of the most important environmental and commercial applications of PolSAR systems is the vegetation monitoring. One of the vegetation monitoring tools is the use of the Radar Vegetation Index (RVI) to extract important information regarding the crops, forests and grasslands. The RVI, as firstly introduced in [5], is a measure of volume scattering (from randomly oriented dipoles), which is a scattering mechanism usually caused by the structural elements of vegetation (leaves, branches and trunks). The RVI can be physically interpreted as proportional to the ratio between the power caused by volume scattering due to vegetation to the total scattered power represents the brightness of an illuminated area on the ground surface. The RVI can be considered a measure of cross polarization due to volume scattering and it has been proposed as a method for monitoring the level of vegetation growth. High correlation exists between RVI with crop age and crop biomass [6]. It ranges between 0 and 1 with

[1] Microwave Engineering Department, Electronics Research Institute, Cairo, Egypt. [2] Electronics and Electrical Communications Department, Faculty of Engineering, Al-Azhar University, Cairo, Egypt.

a value near 0 for a smooth bare soil surface and increases with vegetation growth [7]. The RVI has been introduced in [8] and has been applied in [9] for estimating the Vegetation Water Content (VWC) of rice crop and soybean. It has been found the RVI can be significantly correlated to VWC [10] and Leaf Area Index (LAI). Moreover, the RVI can be correlated to the Normalized Difference Vegetation Index (NDVI) measured by optical sensors at various frequencies [9].

The natural pasture which plays a great role in the economic life (grass can be a main source of food) and ecosystem balance (grassland contributes to carbon storage). The method described in the present paper to recover the grass height from the RVI data collected by a PolSAR system is proposed for the grassland type in which *the vertical orientation of an individual leaf is rather dominant.* If the angle between the leaf and the gravity direction is θ_g then the mean value of this angle is $\mu_{\theta_g} = 0$, whereas its standard deviation σ_{θ_g} is usually very small ($\sigma_{\theta_g} < 10$). This is true for the most common types of natural pasture and, hence, the proposed method is applicable for the estimation of the height of the most commonly types of grasslands.

The present work aims to monitor the natural grass height in a grassland area using the RVI which is calculated using the backscatter coefficients measured by PolSAR systems. For this purpose, electromagnetic (EM) simulation is applied by subjecting realistic geometric models of random strip-wire structures representing the grassland to incident plane waves polarized so as to evaluate the backscatter coefficients. The present work proposes a new geometric model for the natural vegetation covers on the ground surface. In literature, vegetation is usually modeled as clouds of randomly oriented straight dipoles [11–13]. In fact, the long narrow leaves constituting the grass cloud are not straight in shape. It may be more appropriate to use a randomly oriented curly narrow strip as a model for a single leaf of the grass instead of using a thin straight wire with random orientation. Thus, for EM simulation of volume scattering, clouds of conductive random curly strips are used to model grassland areas. EM is achieved by subjecting such grassland models to horizontally polarized and vertically polarized plane waves and then applying the method of moments (MoM) to solve an electric field integral equation (EFIE) to estimate the volume scattering. This is applied to evaluate the scattering from ensembles of grassland models with different grass heights. In this way the relation between the grass height and the corresponding RVI can be obtained. The inverse operation of retrieving the grass height from the measured values of the RVI can be applied and the accuracy of the retrieved grass height is assessed. Figure 1 shows a block diagram for the proposed operation to estimate the grass height through EM simulation. This operation is carried out through a sequence of steps starting with generating multiple geometric models for grassland areas with different values of the grass height. The EM simulation is then applied to obtain the backscatter coefficients from which the RVI can be calculated for the corresponding grass height. The relation between the RVI and the corresponding grass height is obtained as higher-order polynomial. Finally, the inverse operation of estimating the grassland height from the fitted higher-order polynomial is accomplished. The accuracy of the retrieved height is calculated as the difference between the grass height of the geometric model subjected to EM simulation and the height estimated trough the fitted polynomial.

The RVI as measured by a PolSAR system can be influenced to a great extent, by some conditions and working parameters such as the ground surface roughness, soil moisture, radar look angle, VWC,
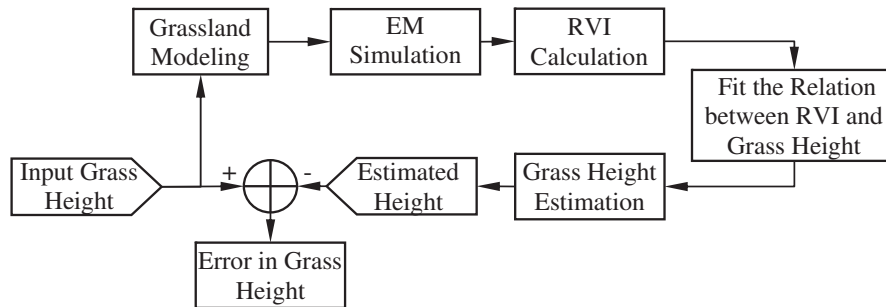

Figure 1. Block diagram for the operation proposed to use EM simulation for estimating the grassland height from the RVI measured by a PolSAR system.

and the vegetation structure itself. Thus, to extract true information from the measured RVI, these conditions and working parameters should be taken into account. Moreover, the speckle noise frequently appearing in SAR data probably results in considerable errors of the RVI from which false information can be estimated [1].

The present work addresses an important problem which may result in significant errors and consequent wrong estimations from the RVI measured by PolSAR systems for grassland areas. The cloud of long narrow leaves constituting a grassland area usually contains quasi-parallel leaves, which may cause dramatic changes of the measured RVI over narrow intervals of the frequency depending on the grass height. This can be more explained in view of the geometric model of the grassland area proposed above. The resonant modes of parallel twins (two-wire) waveguide resonator may probably exist at random positions of the grassland area causing dramatic changes of the backscattered field (peaks or anti-peaks) over very narrow bands of the frequency. As the backscatter coefficients are used to calculate the covariance matrix and, hence, the RVI, it is important to study the conditions of generating such type of resonant modes in a random strip clouds and to investigate their effects on the measured RVI. Unlike the natural modes of a wire, these modes cannot be generated on the surface of a single strip wire and are only generated between couples of wires and, hence, they are named "internal resonances".

The next section of the present paper is concerned with the definition of the RVI, and Section 3 gives a brief note about the resonances of the parallel wires. Section 4 describes the geometric model proposed for the grassland area. Section 5 explains the EM simulation of the PolSAR imaging operation to estimate the RVI. Finally, Section 6 presents and discusses the numerical results concerned with the grassland modeling, EM scattering, calculated RVI, estimated grass height, and the error of the estimated height due to the effect of the internal modes.

2. VEGETATION MONITORING USING SPACEBORNE LAND IMAGING SYSTEMS

Quantitative indices are used to monitor vegetation growth on the earth surface. The most commonly used vegetation monitoring indices are the Normalized Difference Vegetation Index (NDVI) and the RVI. The former is used by spaceborne land-imaging systems based on optical sensors whereas the latter is used by spaceborne PolSAR systems for earth remote sensing. However, the RVI used by PolSAR systems to monitor vegetation growth can be superior to the NDVI as it has low sensitivity to changes in environmental conditions.

2.1. Optical Sensors for Vegetation Monitoring

The NDVI reveals some information about photosynthetic activity and cellular structure of vegetation in a single numerical value. In other words, it is easy to use and understand. NDVI quantifies vegetation by measuring the difference between near-infrared (which vegetation strongly reflects) and red light (which vegetation absorbs).

$$\text{NDVI} = \frac{\text{NIR} - \text{RED}}{\text{NIR} + \text{RED}} \tag{1}$$

Of course there are some limitations in what NDVI can really reveal vegetation structure, but it is a good tool if the available spectral bands are only the red and near infrared bands.

2.2. PolSAR Systems for Vegetation Monitoring

For calculating the RVI, the PolSAR system collects the co-polarized and cross-polarized backscattering coefficients S_{hh}, S_{vh}, S_{hv}, and S_{vv}, which are defined as,

$$S_{hh} = \frac{E_h^r}{E_h^i}\bigg|_{E_v^i=0}, \quad S_{vh} = \frac{E_v^r}{E_h^i}\bigg|_{E_v^i=0}, \quad S_{vv} = \frac{E_v^r}{E_v^i}\bigg|_{E_h^i=0}, \quad S_{hv} = \frac{E_h^r}{E_v^i}\bigg|_{E_h^i=0} \tag{2}$$

where E^i and E^r denote incident and received fields, respectively.

For monostatic PolSAR systems, the EM reciprocity implies that $S_{hv} = S_{vh}$, and hence, the covariance matrix can be assessed as follows, where operator $\langle\rangle$ denotes the ensemble average, while superscript $*$ denotes the complex conjugate.

$$\langle[C]\rangle = \begin{bmatrix} \sigma_{hh}^2 & \sqrt{2}\sigma_{hh,hv} & \sigma_{hh,vv} \\ \sqrt{2}\sigma_{hv,hh} & 2\sigma_{hv}^2 & \sqrt{2}\sigma_{hv,vv} \\ \sigma_{vv,hh} & \sqrt{2}\sigma_{vv,hv} & \sigma_{vv}^2 \end{bmatrix} = \begin{bmatrix} \langle|S_{hh}|^2\rangle & \sqrt{2}\langle S_{hh}S_{hv}^*\rangle & \langle S_{hh}S_{vv}^*\rangle \\ \sqrt{2}\langle S_{hv}S_{hh}^*\rangle & 2\langle|S_{hv}|^2\rangle & \sqrt{2}\langle S_{hv}S_{vv}^*\rangle \\ \langle S_{vv}S_{hh}^*\rangle & \sqrt{2}\langle S_{vv}S_{hv}^*\rangle & \langle|S_{vv}|^2\rangle \end{bmatrix} \quad (3)$$

where σ_{hv}^2 is the variance of S_{hv}, and σ_{hh}^2 and σ_{vv}^2 are the variances of S_{hh} and S_{vv}, respectively, expressed in power unit.

RVI is a simple function of radar backscatter coefficients, which includes a unique combination of all polarizations. Using elements of the covariance matrix defined in Eq. (3), the RVI can be calculated as follows

$$\text{RVI} = \frac{8\sigma_{hv}}{\sigma_{hh} + \sigma_{vv} + 2\sigma_{hv}} \quad (4)$$

The denominator of the quantity on the right-hand-side of Eq. (4) can represent the total scattered power from the illuminated target area. Thus, the RVI can be physically interpreted as proportional to the ratio of the power caused by volume scattering due to vegetation to the total scattered power which represents the brightness of an illuminated area on the ground surface. RVI is a measure of the cross-polarization of backscatter from PolSAR targets. For sea surface and desert or bare lands, RVI is usually less than 0.2. For natural vegetation areas, RVI ranges from 0.2 to 1.0. For urban areas and man-made structures, RVI is usually greater than 1.0.

3. INTERNAL RESONANCES OF RANDOM WIRE STRUCTURES

Long narrow leaves constituting the grassland may contain many pairs of quasi-parallel leaves. It may be useful to study the behavior of such resonant modes generated between couples of parallel straight as well as random curly wires. To account for the generation of such internal resonances in the EM simulation, the modes of the two-strip waveguide resonator are discussed. The two-strip transmission line has a principal TEM mode with zero cutoff frequency. Like cavity-backed apertures [14, 15], the
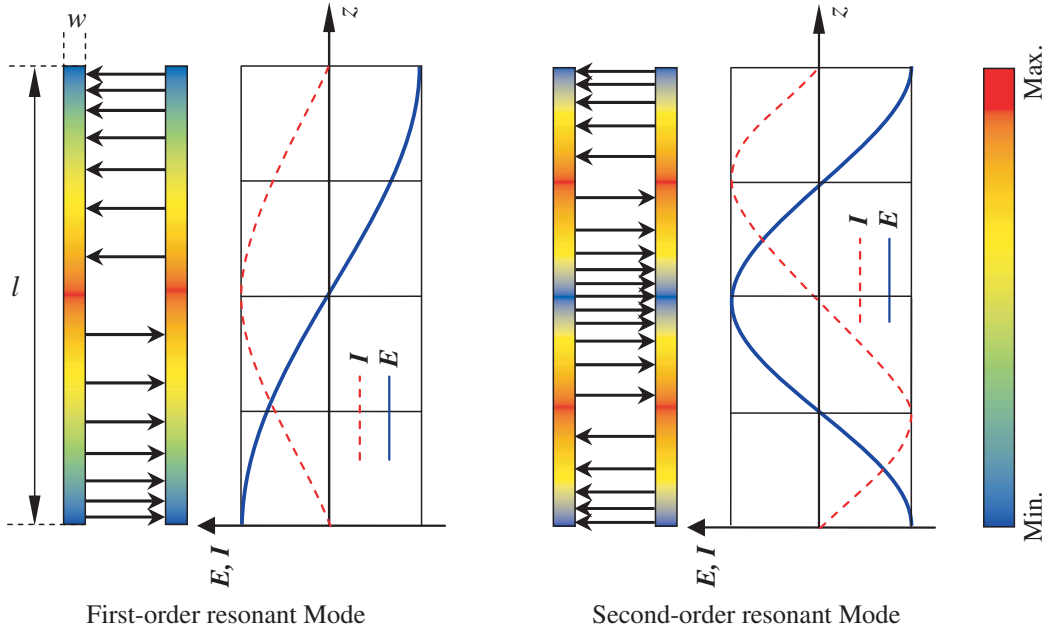

Figure 2. Distribution of the current on the strip surfaces and the electric field between the two-strip waveguide at the first and second resonant modes.

finite length open ended two-wire transmission line has (internal) resonant modes. For very narrow strips $(w/L \rightarrow 0)$, the resonant frequencies of the resonant TEM modes of the two-strip waveguide resonator can be calculated as follows.

$$f_n^{\text{TEM}} \approx \frac{c}{\lambda_n^{\text{TEM}}} \approx n\frac{c}{2L}, \quad n = 1, 2, 3, \ldots \tag{5}$$

where λ_n^{TEM} is the wavelength of the two-wire TEM guided mode, c the velocity of light, L the length of the two-wire transmission line, and n the order of the resonant mode.

Figure 2 shows the current distribution on the surface of the strips and the electric field lines in the region between the parallel strips at the frequencies corresponding to the first and second internal resonances. It should be noticed that natural resonances of a narrow straight strip occur at frequencies given by the same expression as Eq. (5). This means that a pair of parallel strips is characterized by both internal (waveguide) resonant modes and external (natural) resonant modes occurring at almost the same resonant frequencies.

4. MODELING OF NATURAL GRASSLAND AS CLOUDS OF CONDUCTIVE RANDOM CURLY STRIPS

For electromagnetic simulation, natural vegetation covers on the ground surface are usually modeled in literature as random structures composed of randomly oriented and distributed straight wires. Nevertheless, the long narrow leaves constituting the grass cloud are not usually straight. Therefore, instead of using randomly oriented thin straight wires for electromagnetic simulation of volume scattering from vegetation areas, the present work proposes a random curly conductive strip to be used as a model for a single leaf of the grass.

The long narrow leaf of the grass has height h and width w which are random variables with normal distributions within a cloud of leaves constituting a grassland area. In the present study, such a leaf is geometrically modelled as a curly strip constructed of pairs of vertices. The vertices of a pair have the
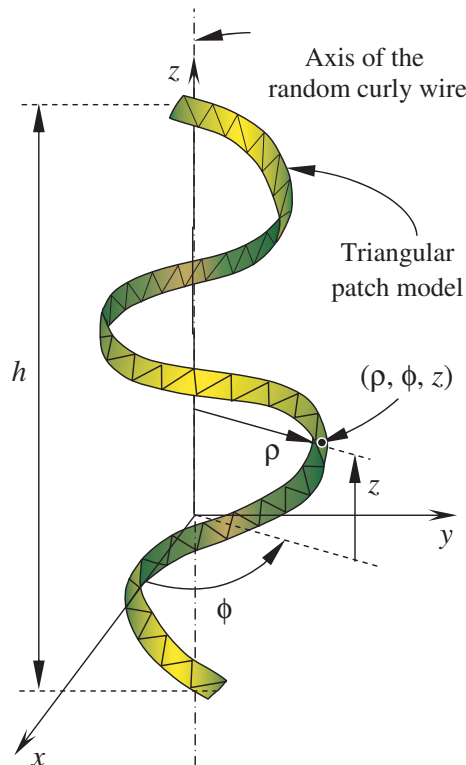

Figure 3. Triangular patch model of random curly strip with its geometrical parameters.

same z-coordinate and are horizontally separated by distance w. The centerline of the strip is discretized to a number of M points which are sequentially connected for $m = 1, 2, ..., M$. The coordinates of each point are (ρ_m, ϕ_m, z_m). Once the strip height h is determined, the points on the center line of the strip are uniformly distributed along the strip axis with their z-coordinates given as follows.

$$z_m = (m-1)\frac{h}{M}, \quad m = 1, 2, 3, ..., M \tag{6}$$

The coordinates ρ_m and ϕ_m are Gaussian random numbers with mean values μ_ρ and μ_ϕ, respectively and standard deviation, σ_ρ and σ_ϕ, respectively. The random numbers ρ_m and ϕ_m for $m = 1, 2, ..., M$ are spatially correlated along the z-axis with correlation length $l_{\rho c}$ and $l_{\phi c}$, respectively. The random values of ρ_m and ϕ_m are generated using the Savitzky-Golay filter method described in [16] for generating one dimensional sequence of spatially correlated random numbers.

Both parameters of the geometric model of each strip and the statistical parameters that control the distribution of the strips within the random cloud should be set to match the type of grass subjected to EM simulation. Figure 4(a) shows a random curly strip which can be an element of a random cloud, whereas Figure 4(b) shows a cloud of such random curly strips to simulate natural grassland area for realistic EM simulation of the PolSAR system operation.
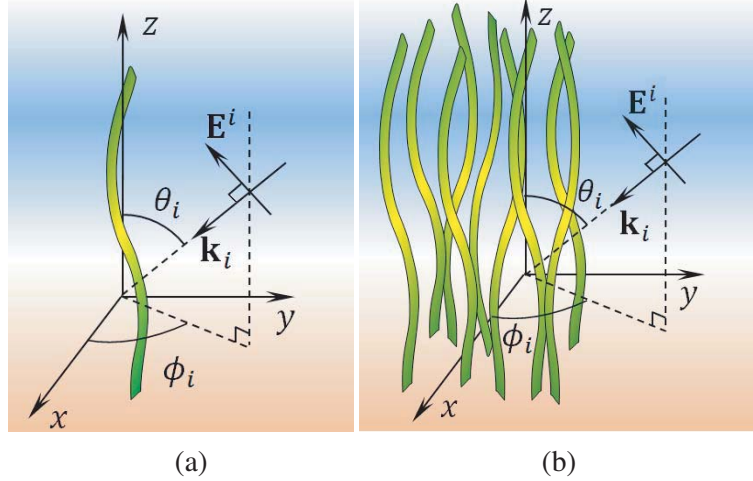

Figure 4. Geometric models of single random curly strip and a random cloud of such a strip subjected to incident plane waves for EM simulation. (a) Single random curly strips. (b) Cloud of random curly strips.

Models of vegetation areas are constructed as clouds of random curly strips with statistical properties that ensure accurate representation of the natural grassland areas. A random volumetric structure of such random curly strips can be constructed as shown in Figure 4(b) by generating a number of these strips, each at a location defined by the random variables (x_o, y_o, z_o) which are normally distributed with mean values μ_{xo}, μ_{yo}, and μ_{zo}, respectively, and standard deviations σ_{xo}, σ_{yo}, and σ_{zo}, respectively. It should be noted that the mean values and variances of these coordinates are arbitrarily determined according to the horizontal density of the natural grass. Since the vertical orientation of an individual leaf is rather dominant for most of the grassland types, the angle between the leaf and gravity direction, θ_g, should have Gaussian probability distribution function. Assuming no wind conditions, the mean value of this angle is $\mu_{\theta_g} = 0$, whereas its standard deviation σ_{θ_g} is usually very small ($\sigma_{\theta_g} < 10$) for most of the grassland types. When such a grassland area is subjected to a plane wave incident at an angle θ_i with the vertical direction (z-axis), the aspect angles for the leaves of the grass can be considered as Gaussian random variable θ_A, whose mean value is $\mu_{\theta_A} = \theta_i$ and standard deviation $\sigma_{\theta_A} = \sigma_{\theta_g}$.

To demonstrate the effect of the internal resonances on the RVI assessed through EM simulation, two models of grassland areas are generated: model A and model B. The grassland model A is free from internal resonances. To prevent the generation of such resonances within model A when it is subjected

to incident plane wave, no pair is allowed to have its strips parallel. On the other hand, grassland model B is allowed to excite internal resonances. This is achieved by constructing such a model using a cloud of randomly oriented pairs of axially-parallel curly strips, where each individual strip has the same statistical parameters as that used to construct grassland model A. The pairs of curly strips of model B are randomly oriented and have their aspect angles following the same distribution as that of grassland model A. It should be noted that both models A and B should have the same number of curly strips.

5. ELECTROMAGNETIC SIMULATION OF POLSAR IMAGING AND ESTIMATION OF RADAR VEGETATION INDEX

A single strip or a cloud of strips can be subjected to incident plane wave of specific polarization to simulate the PolSAR operation during land imaging. The operation of land imaging through monostatic side-looking PolSAR can be simulated as a spaceborne (satellite) antenna moving in the azimuth direction at altitude H as shown in Figure 5. This antenna continuously transmits electromagnetic pulses at a specific rate. Each pulse can be considered as a pulsed plane wave incident on the ground at an angle θ_i with the satellite nadir. The ground range direction is parallel to the ground surface and normal to the azimuth direction as shown in the figure.
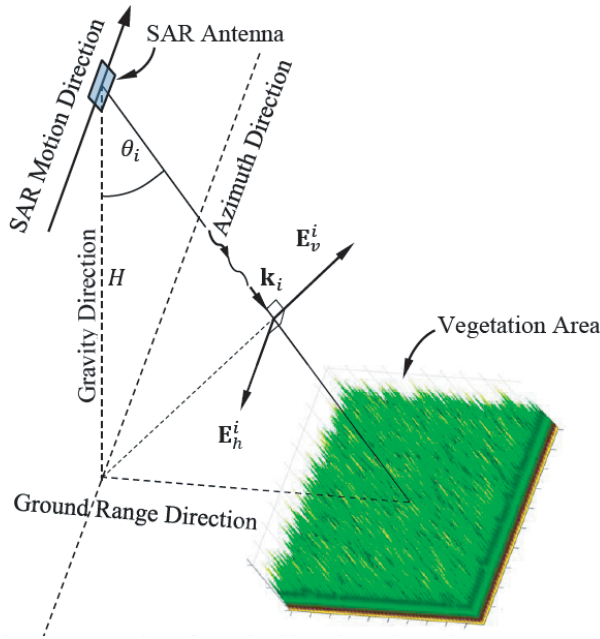

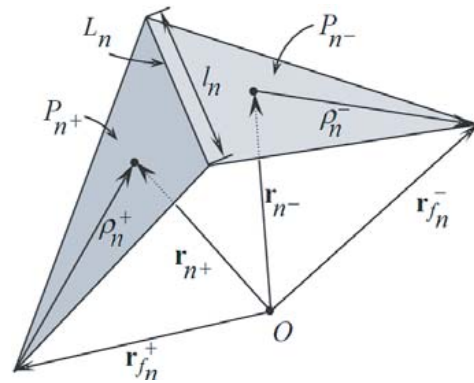**Figure 5.** Operation of grassland imaging using PolSAR system.

Figure 6. Basis function for surface current expansion on two triangles sharing an edge [17].

For obtaining backscatter coefficients, it is required to deduce the current flowing on the strip surface due to an incident plane wave. As shown in Figure 3, the strip surface is divided into a number of triangular patches, and each has three edges; an edge which belongs to only one triangular patch is called a *boundary edge*. Such an edge exists only on the rim of the surface, and hence, it has no electric current component flowing normal to it. An edge which belongs to two triangular patches is a *non-boundary edge*. The current flowing on the conducting surface is expressed as a summation of vector basis functions with unknown amplitudes as given by Eq. (7). Each basis function is defined for a pair of triangular patches sharing a none-boundary edge. The most suitable basis function may be the Rao-Wilton-Glisson (RWG) basis function [17]. Figure 6 shows two triangular patches sharing a non-boundary edge on which the basis function is defined.

The current distribution, $\mathbf{J}$, flowing on the strip surface can be expanded in terms of the RWG basis functions as follows.

$$\mathbf{J} = \sum_{n=1}^{N} I_n \mathbf{f}_n, \tag{7}$$

where I_n is the magnitude of the current crossing the edge L_n, and $\mathbf{f}_n$ is the RWG basis function defined as follows.

$$\mathbf{f}_n = \begin{cases} \dfrac{l_n}{2S_{n^+}} \boldsymbol{\rho}_n^+, & \mathbf{r} \in P_{n^+} \\ \dfrac{l_n}{2S_{n^-}} \boldsymbol{\rho}_n^-, & \mathbf{r} \in P_{n^-} \\ 0, & \text{otherwise} \end{cases} \tag{8}$$

where $\boldsymbol{\rho}_{n^+}$ is the triangular patch from which the current is flowing out, and $\boldsymbol{\rho}_{n^+}$ is the triangular patch to which the current is flowing in.

l_n is the length of the non-boundary edge L_n, $\mathbf{r}$ the position vector of a point in one of the two triangles, $S_{n^\pm}$ the area of $P_{n^\pm}$, and vector $\boldsymbol{\rho}_n^\pm$ is given as follows.

$$\boldsymbol{\rho}_n^\pm = \pm \left(\mathbf{r}_{n^\pm} - \mathbf{r}_{f_n}^\pm \right), \tag{9}$$

The scattered electric field is expressed as an integral of the unknown current flowing on the strip surface. The boundary conditions are applied to enforce vanishing of the tangential electric field on the conducting surface. Thus, an EFIE is formulated for the unknown current magnitude, I_n. Once the EFIE is formed, it can be solved using the MoM to get the unknown current distribution on the strip surface. Consequently, the backscattered far field can be evaluated by simulation of two cases: (i) the incident plane wave is horizontally polarized ($E_v^i = 0$) and (ii) the incident plane wave is vertically polarized ($E_h^i = 0$) giving rise to the coefficients S_{hh}, S_{hv}, S_{vh} and S_{vv} given by Eq. (2).

6. RESULTS AND DISCUSSION

In the present section, the numerical results for geometric models of the clouds representing grassland areas are presented. The RVI is calculated through EM simulation by subjecting the random strip clouds to both horizontally polarized and vertically polarized plane waves. A quantitative estimation of the grass height is achieved by fitting the relation between the RVI and grass height as a higher-order polynomial which accurately expresses the grass height as a single-valued function of the RVI. The effect of the peaks or anti-peaks that appear in the collected RVI data with changing the grass height due to the internal resonances of the strip cloud is investigated. The consequent errors encountered in the estimation of the grass height are numerically evaluated under some conditions of the internally resonant modes.

6.1. Geometric and Electric Models of Grassland Using Random Strip Structures

To study the characteristics of electromagnetic scattering from vegetation or natural grassland, models of random strip structures are constructed. By controlling the statistical parameters of the random curly strip shown in Figure 3, the long narrow leaves constituting the grass land can be accurately simulated. The current section presents geometrical models of a random curly strip and random clouds of such a strip.

6.1.1. Geometric Modelling of Random Curly Strip

To be used as a constituent of a grassland model, a random curly strip of height $h = 20\,\text{cm}$ can be modeled as described in Section 4, Figure 3, with different values of the statistical parameters: μ_ρ, σ_ρ and μ_ϕ, σ_ϕ. Samples of such random curly strips are presented in Figure 7.
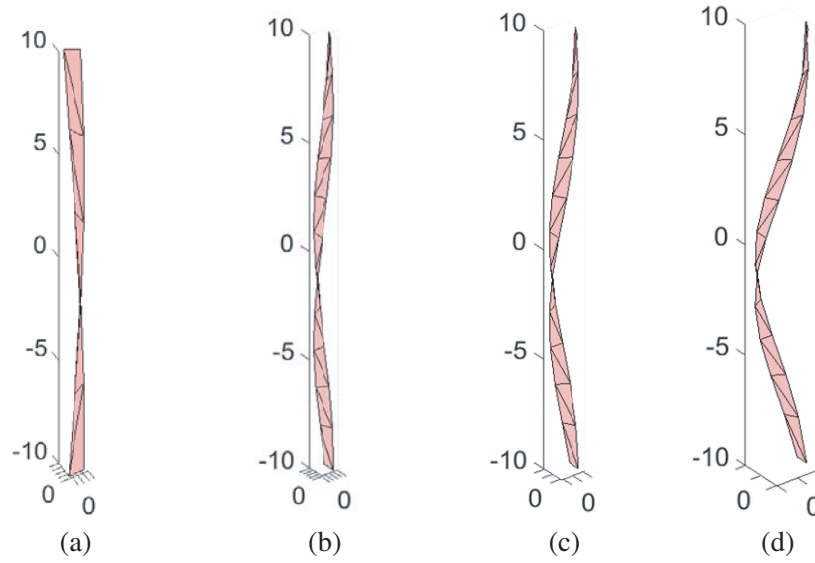
Figure 7. Triangular patch models of random curly strips of height $h = 20\,\text{cm}$ and $w = 0.3\,\text{cm}$ with different values of μ_ρ and μ_ϕ. (a) $\mu_\rho = 3\,\text{mm}$, $\mu_\phi = 90°$ and $\sigma_\phi = 45°$. (b) $\mu_\rho = 3\,\text{mm}$, $\mu_\phi = 180°$ and $\sigma_\phi = 90°$. (c) $\mu_\rho = 5\,\text{mm}$, $\mu_\phi = 180°$ and $\sigma_\phi = 90°$. (d) $\mu_\rho = 1\,\text{cm}$, $\mu_\phi = 180°$ and $\sigma_\phi = 90°$.

6.1.2. Clouds of Random Curly Strips for Grassland Modeling

This section presents random clouds of curly strips as described in Section 4. Figures 8(a), (b) show three different models of the grassland areas constructed as random curly strips with mean height $\mu_h = 5\,\text{cm}$ and $30\,\text{cm}$, respectively. For the three grassland areas, the individual strip has the following statistical parameters $\mu_\rho = 3\,\text{mm}$, $\sigma_\rho = 0.5\,\text{mm}$, $l_{\rho c} = 20\,\text{cm}$, $\mu_\phi = 90°$, $\sigma_\phi = 45°$ and $l_{\phi c} = 20\,\text{cm}$. The area over which the cloud is constructed is $50\,\text{cm} \times 50\,\text{cm}$ including total number of 2500 strips with average spacing of $1\,\text{cm}$. Each of the ($50\,\text{cm} \times 50\,\text{cm}$) models of the grassland areas presented in Figure 8 can be used to represent a homogeneous natural grassland area corresponding to a pixel in a PolSAR image of resolution $0.5\,\text{m} \times 0.5\,\text{m}$.
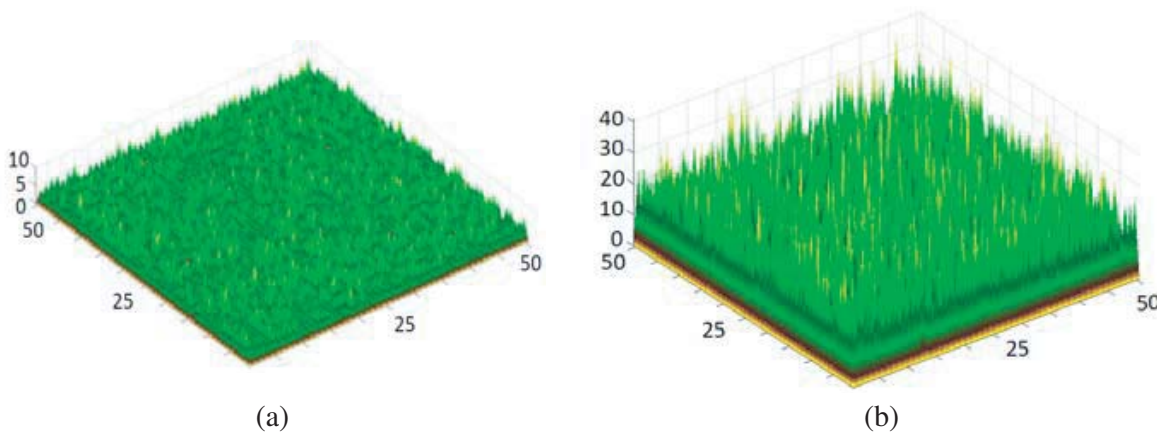

Figure 8. Two grassland models each of $50\,\text{cm} \times 50\,\text{cm}$ using volumes of random curly strips. (a) $\mu_h = 5\,\text{cm}$ and $\sigma_h = 1.5\,\text{cm}$. (b) $\mu_h = 30\,\text{cm}$ and $\sigma_h = 3\,\text{cm}$.

Each of the individual strips composing the cloud is randomly oriented to have its axis in the direction (θ_g, ϕ_g). Angle ϕ_g is a random variable with uniform distribution such that $\phi_g \in \{0, 360°\}$. Angle θ_g is a Gaussian random variable with mean μ_{θ_g} and standard deviation σ_{θ_g}. To get almost all

the strips of the generated cloud oriented so as to satisfy the condition $\theta_{\min} < \theta_g < \theta_{\max}$, the standard deviation should be set as follows $\sigma_{\theta_g} = (\theta_{\max_g} - \theta_{\min_g})/6$. As the vertical orientation is dominant for a leaf of the grass one may confine θ_g to the closed interval: $\theta_g \in [-15°, 15°]$; this means to set $\mu_{\theta_g} = 0$ and $\sigma_{\theta_g} = (15 - (-15))/6 = 5°$. The angle ϕ_g is a random variable with uniform distribution such that $\phi_g \in \{0, 360°\}$.

The geometric model of a grassland area corresponding to a pixel in a PolSAR image of resolution $1\,\mathrm{m} \times 1\,\mathrm{m}$ can be constructed as a $1\,\mathrm{m} \times 1\,\mathrm{m}$ square area within which the strips are randomly distributed according to either model A or model B. To get an average distance about $4\,\mathrm{cm}$ between the neighboring leaves, the density of the leaves of the grassland area is set to $720\,\mathrm{leaf}/\mathrm{m}^2$. For such a grassland area with model A, the orientation, θ_g, of each strip follows the Gaussian distribution shown in Figure 9. For numerical simulation it may be convenient to discretize the random variable θ_g so that it takes one of seven values as follows: $\theta_g \in \{-15, -10, -5, 0, 5, 10, 15\}$. In this case, the discretized Gaussian distribution shown in Figure 9 as a bar chart can be used to create the geometric model of the grassland area. This can be explained more in view of Table 1, which shows the number of strips having a certain vertical orientation (specific value of θ_g).

This means that, for a plane wave incident at angle θ_i with the vertical direction, the individual strips have their aspect angles $\theta_A = \theta_i + \theta_g$ as a random variable of Gaussian distribution with mean, $\mu_{\theta_A} = \mu_{\theta_g} + \theta_i$, and standard deviation, $\sigma_{\theta_A} = \sigma_{\theta_g}$.

For example, if the plane wave is incident at $\theta_i = 40°$, on a grass of $\mu_{\theta_g} = 0$, and $\sigma_{\theta_g} = 5°$, the aspect angle θ_A is confined in the range $\theta_A \in [25°, 55°]$, which means $\mu_{\theta_A} = 40°$ and $\sigma_{\theta_A} = 5°$.
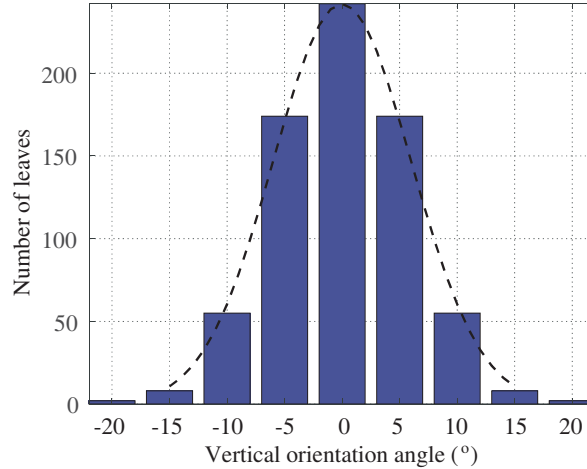

Figure 9. Evaluation of the weights of the ensemble averaging over the aspect angles.

Table 1. The number of strips having a certain vertical orientation (specific value of θ_g) for a cloud of 720 strips representing a $1\,\mathrm{m} \times 1\,\mathrm{m}$ grassland area of either model A or model B with average horizontal separation of about $4\,\mathrm{cm}$ between the leaves of the grass.

θ_g	$-15°$	$-10°$	$-5°$	$-0°$	$5°$	$10°$	$15°$	Total number of strips/strip couples
Number of strips (model A)	9	59	172	238	172	59	9	720
Number of strips couples (model B)	5	30	85	119	85	30	5	360

6.2. Estimation of the RVI through Electromagnetic Simulation

For electromagnetic simulation, consider a SAR image with resolution $1\,\text{m} \times 1\,\text{m}$ (the ground surface area corresponding to a pixel). As the SAR data are collected for each pixel, it is required to construct geometric models for grassland areas with dimensions $1\,\text{m} \times 1\,\text{m}$ for each area as described in Section 4.

The aspect angle, θ_A, is the angle between the direction of incidence of the plane wave and the axis of a strip in a cloud representing the grassland can be considered as a Gaussian distributed random variable. For a plane wave incident at angle θ_i, the mean value of θ_A, μ_{θ_A} is equal to θ_i. The standard deviation of θ_A, σ_{θ_A} is a measure of the scatter of the strips constituting the grass model. To simulate natural pasture, it may be appropriate to set $\sigma_{\theta_A} = 7°$. To get realistic simulation of the back scattering coefficients for natural grassland the variation of θ_A among the constituent strips of the grass model should be taken into consideration. For a SAR look angle $\theta_i = 40°$, the electromagnetic simulation is achieved for the seven values of the aspect angle: $\theta_A = 25°$, $30°$, $35°$, $40°$, $45°$, $50°$, and $55°$. Such sample values of θ_A are taken to satisfy an average $\mu_{\theta_A} = 40°$. Thus, an ensemble of 7 samples of random curly clouds for each of the indicated aspect angles is created. The backscattering coefficients S_{hh}, S_{vh}, S_{hv}, and S_{vv} are evaluated for each sample of the grass land models and averaged considering the Gaussian distribution of θ_A. That is the weights of the averaging are Gaussian distributed with mean value of $\theta_A = 40°$ and standard deviation of $7°$. The variation of the averaged values of the scattering coefficients with the frequency is presented in Figure 10(a). The corresponding covariance matrix is calculated, and hence, the ensemble-averaged RVI is plotted against the frequency as presented in Figure 10(b) with some fitted relations.
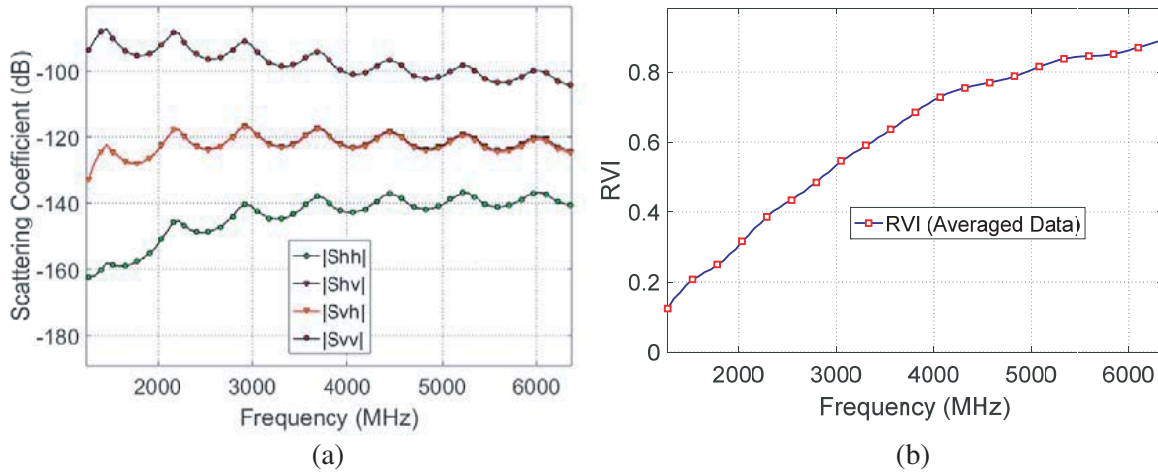

Figure 10. Frequency dependence of the Gaussian weighted average of the backscatter coefficients, S_{hh}, S_{vh}, S_{hv}, and S_{vv} and the corresponding RVI where the averaging is performed over different values of the aspect angle (θ_A).

6.3. RVI as a Monitor for Grass Height

The covariance matrix is calculated using the ensemble-averaged values of the scattering coefficients obtained through EM simulation for a SAR look angle of $40°$. Hence, the relation between the ensemble-averaged RVI for the 70 ensembles and the grass height can be obtained as presented in Figure 11. Curve fitting using a 5th-order relation can be calculated to get the inverted relation from which the grass height can be accurately estimated using the RVI data obtained through EM simulation. The fitted 5th-order polynomial is given by Eq. (10), and the corresponding fitted curve is plotted in Figure 11.

$$L_g = 673(\text{RVI})^5 - 1083(\text{RVI})^4 + 612(\text{RVI})^3 - 125(\text{RVI})^2 + 68(\text{RVI}) + 12.19, \quad \begin{aligned} 0 \leq \text{RVI} \leq 0.89, \\ 20 \leq L_g \leq 100 \end{aligned} \quad (10)$$
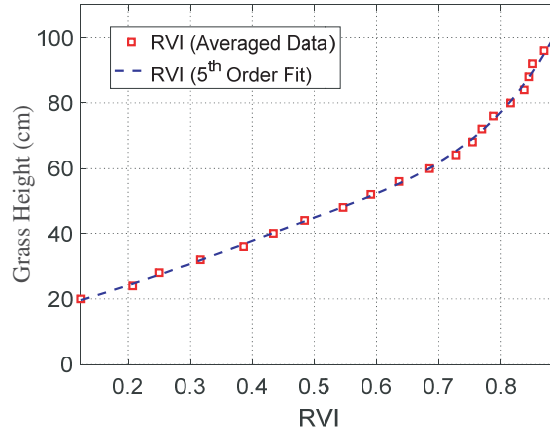
Figure 11. The Gaussian weighted ensemble-average of the RVI against grass height, SAR look angle, $\theta_i = 40°$.

As the grassland models and EM simulation are realistic, the relation in Eq. (10) or, equivalently, the curve plotted in Figure 11 can be considered as a reference to estimate the grass height from the RVI data collected by an actual PolSAR system providing that the grass height lies in the range: $20 \le L_g \le 100$, and the RVI lies in the range: $0 \le \text{RVI} \le 0.89$.

6.4. Resonant Modes of Finite-Length Two-Strip Waveguide

The RCS of a pair of parallel straight strips is investigated over a wide frequency range. For this purpose, two parallel strips of length 20 cm and 4 cm apart are subjected to a vertically polarized incident plane wave as shown in Figure 12(a). The RCS of such a strip structure is plotted against the frequency as shown in Figure 12(b) and compared with the RCS of a single strip of the same length. As shown in the figure, the RCS of the two-strip structure has sharp peaks over very narrow bands of the frequency. Such peaks do not appear in the frequency response of the RCS of the single wire. Consequently, such sharp peaks occur at resonant frequencies corresponding to the modes generated between the couple
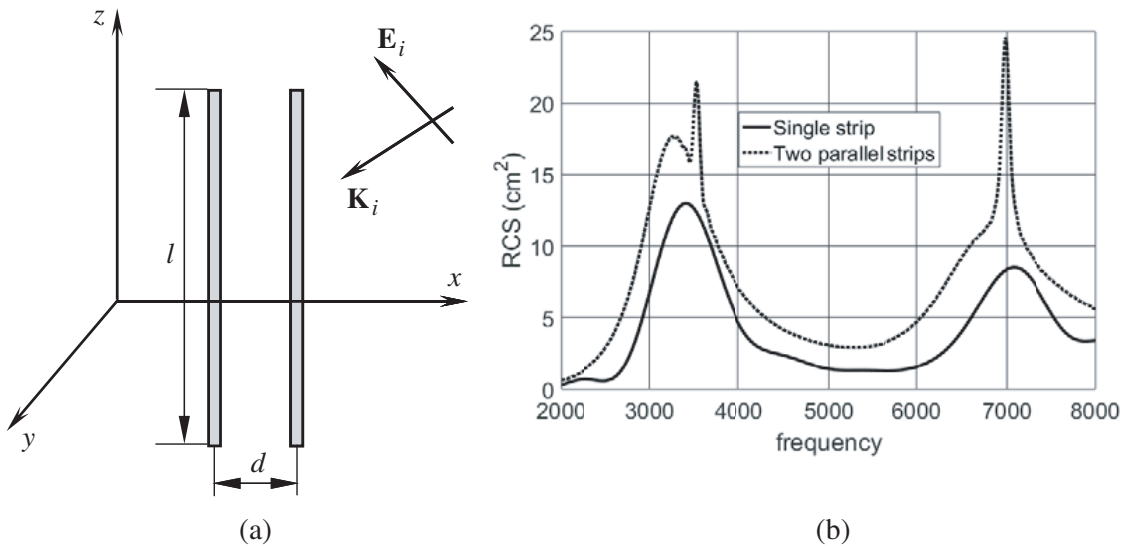

(a)   (b)

Figure 12. Two parallel strips ($l = 20$ cm and $d = 4$ cm) subjected to a vertically polarized incident plane wave $\theta_i = 45°$ and $\phi_i = 0°$. (a) Two parallel strip wires. (b) Frequency response of the RCS.

of strips. It is noticed that such internal resonances appear at frequencies near those of the natural modes of a single strip. Thus, the frequency behavior of the RCS of two-strip structure is characterized by wide-band smooth peaks at the natural resonances and narrow-band sharp peaks at the internal resonances.

The near field distributions in the region around the two parallel straight strips are presented in Figure 13 at the frequencies corresponding to first and second natural and internal resonant modes. As shown in Figure 13(a), the electric field at the first natural resonance seems to be bound to each wire as if this wire exists alone, and hence, the field around each individual wire is related to the current distribution on this strip. On the contrary, the electric field at the first internal resonance is concentrated in the area between the two wires as shown in Figure 13(b), which means that the electric field lines are extending between the two wires. Thus, the two strips parallel and close to each other are necessary requirements for such an internal resonance to take place. One can say that a natural resonance can exist even for a single wire whereas an internal resonance requires at least a couple of wires to exist. This can be confirmed by the near field distributions around the same couple of strips at the frequencies corresponding to the second-order natural and internal resonances as shown in Figures 13(c) and 13(d), respectively. It should be noticed that both natural and internal resonances take place when the strip length is nearly integer multiples of half the wavelength of the incident wave as explained in Section 3 and given by Eq. (5). For example, the first and second order natural and internal resonances take place when the strip length is almost equal to $\lambda/2$ and λ, respectively. In conclusion, a pair of conducting strips of finite length can act as a waveguide resonator that has its resonant modes occurring at frequencies determined by the waveguide length (length of the two strips), a fact which is discussed in Section 3.
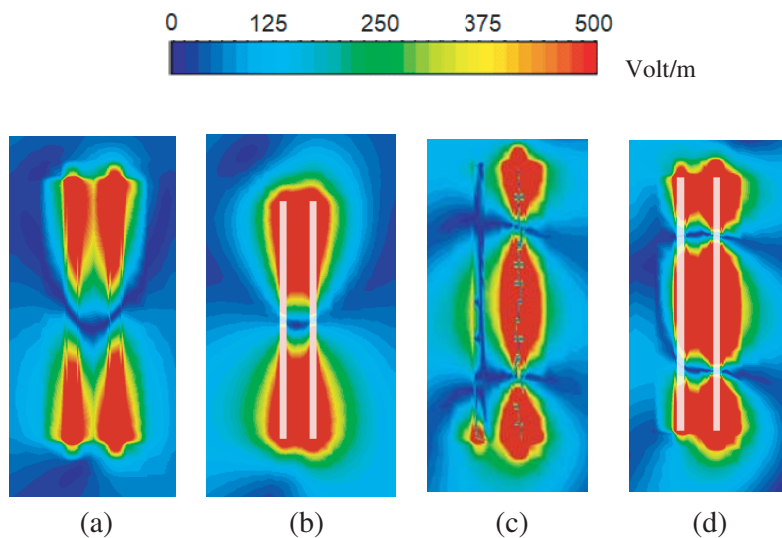

Figure 13. Electric field distribution in the near zone around two parallel wires at natural and internal resonances. (a) 1st natural resonance, $f = 3250\,\text{MHz}$. (b) 1st internal resonance, $f = 3450\,\text{MHz}$. (c) 2nd natural resonance, $f = 6805\,\text{MHz}$. (d) 2nd internal resonance, $f = 6967\,\text{MHz}$.

6.5. Resonant Modes of a Couple of Finite-Length Axially Parallel Random Curly Strips

Like a pair of parallel straight strips with their internal resonant modes discussed in Section 3, a pair of axially-parallel random curly strips can support internal resonant modes. This can be investigated by subjecting a pair of curly strips whose axes are parallel to the z-axis, as shown in Figure 14(a), to a vertically polarized plane wave propagating in the direction $\theta = 45°$. For a structure of two axially parallel random curly strips of the same height, $h = 5\,\text{cm}$ and separated by a distance $d = 1.0\,\text{cm}$, the distribution of the near field is plotted in the region around the two strips as shown in Figures 14(b), (c), (d) at the frequencies corresponding to the first, second, and third order internal resonances. The
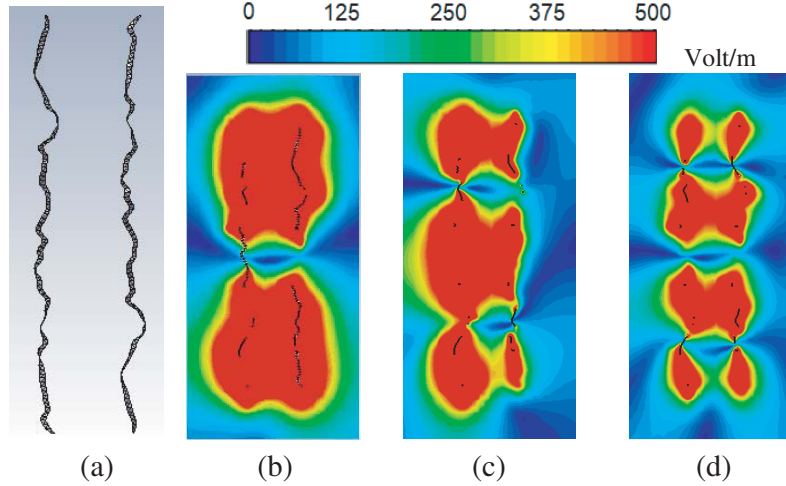
Figure 14. Near field distribution around a couple of axially parallel (z-oriented) curly wires of the same height $h = 5\,\text{cm}$ with their axes separated by distances $d = 1.0\,\text{cm}$. (a) Two curly wires. (b) 1st resonance $f = 2482\,\text{MHz}$. (c) 2nd resonance $f = 4980\,\text{MHz}$. (d) 3rd resonance $f = 7537\,\text{MHz}$.

electric field concentration between the two strips and its variation along the wires exhibits the order of the corresponding internal resonance. It is clear that the near field distribution behaves in a manner similar to that of the near field distribution at the internal resonances of two parallel straight strips presented in Section 6.4. One can conclude that the internal resonances of a pair of axially-parallel random curly strips are almost governed by the same rules as those of the straight strips and can be approximately evaluated using Equation (5).

6.6. Effect of the Internal Resonances of Random Strip Clouds on the RVI

The present section demonstrates and discusses the effects of the internal modes of random clouds of curly strips representing grassland areas on the RVI as measured by PolSAR systems. This is achieved through EM simulation using both vertically and horizontally polarized plane waves incident on the random strip structure with different values of the aspect angle. Figure 15 shows comparisons between the RVI obtained through EM simulation for a single curly strip and that for a pair of axially parallel strips of the same statistical parameters. As shown in the figure, the latter seems to be greatly affected by the internal resonances especially at the resonant frequencies. The sharp peaks (or anti-peaks) appearing in the RVI frequency response for the couple of axially parallel strips do not appear for the single curly strip. Another important fact that can be concluded from the results presented in Figure 15 is that the RVI is strongly dependent on the aspect angle.

The frequency responses of the RVI calculated for realistic grassland clouds (constructed of 720 random curly strips) of both models A and B (as given in Table 1) are presented in Figure 16 for average grass height $h = 20\,\text{cm}$. It is clear that the RVI for grassland model B (including pairs of axially-parallel curly strip wires) has considerable differences compared with that of the grassland model A (of unparalleled curly strips) especially at the frequencies corresponding to the internal resonances. Recall that the RVI can be used as a monitor for the grass height as described in Section 6.3. The comparison between the two curves plotted in Figure 16 shows that the RVI at the internal resonances cannot be considered as an accurate monitor of the grass height using the reference relation given by Eq. (10) or the reference curve presented in Figure 11, especially at the frequencies of the internal modes. Considerable differences may lead to large errors in the inverse process of recovering the grass height due to the occurrence of the internal resonances of the random wire structure representing the grassland model.

The following section is concerned with a quantitative demonstration of the errors encountered during the estimation of the grass height using the RVI due to the effect of internal resonances.
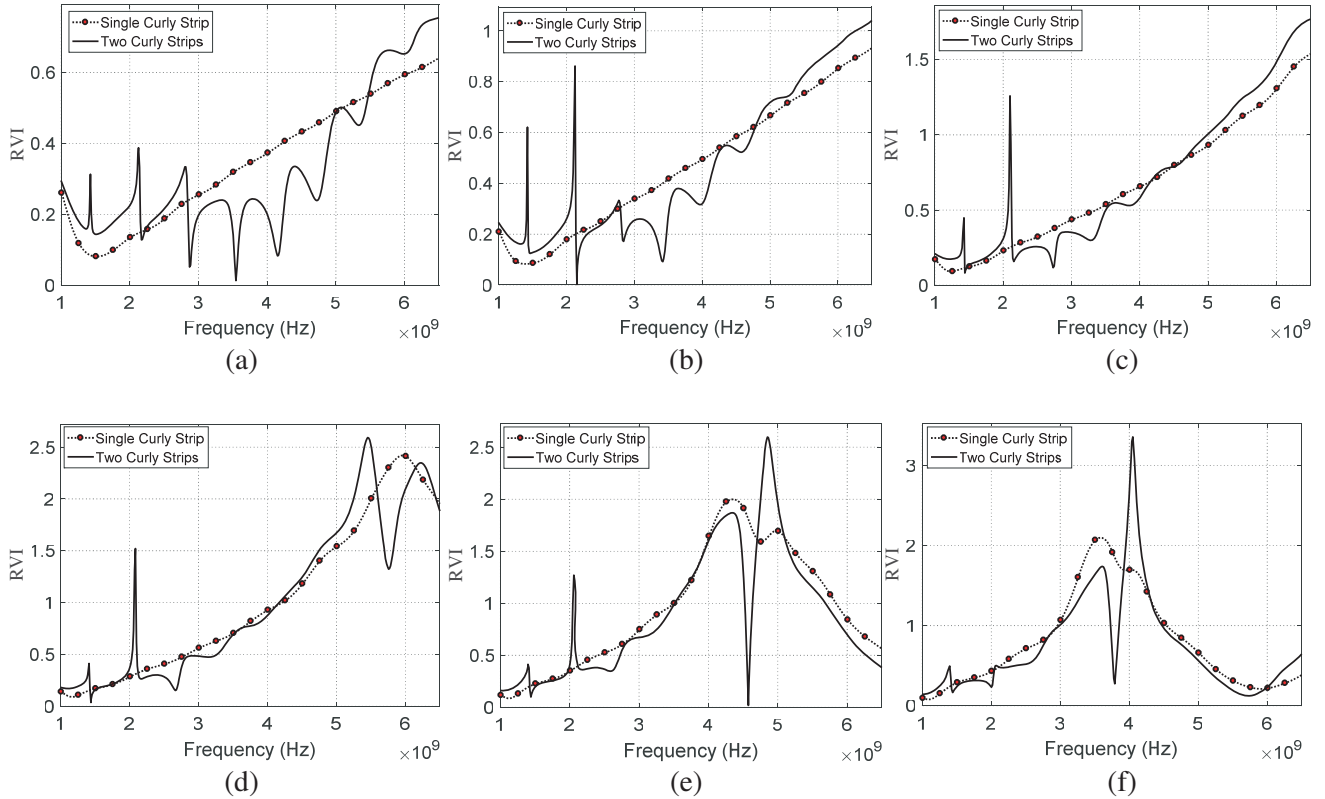
Figure 15. Frequency response of the RVI showing the effect of internal modes through electromagnetic simulation using plane wave incident with different values of the aspect angle θ_i, strip length $l = 20$ cm, width $w = 1$ cm, separation $d = 4$ cm. (a) $\theta_i = 25°$. (b) $\theta_i = 30°$. (c) $\theta_i = 35°$. (d) $\theta_i = 40°$. (e) $\theta_i = 45°$. (f) $\theta_i = 50°$.
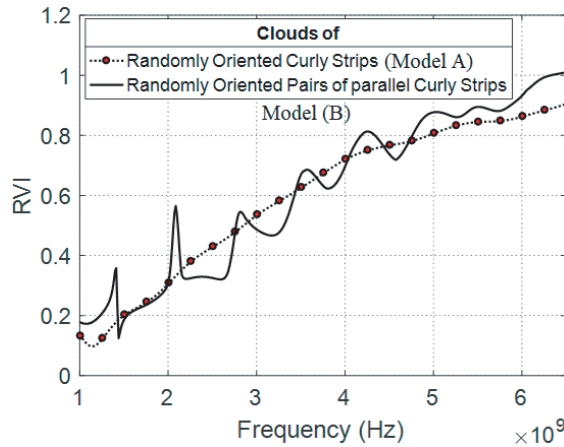

Figure 16. Frequency response of the RVI for random cloude of curly strips showing the effect of internal resonances through electromagnetic simulation strip height $h = 20$ cm, width $w = 1$ mm, separation $d = 4$ cm.

6.7. Errors in Grass Height Estimation due to the Effect of the Internal Resonances

As presented in Section 6.3, the RVI measured by PolSAR systems can be used to monitor the grass height. However, the presence of the internal modes may lead to erroneous recovery of the grass height

due to the singular sharp peaks of the RVI-frequency curve as presented in Figure 16 and discussed in Section 6.6. For quantitative assessment of such errors, grassland model B with intended inclusion of some pairs of axially-parallel curly strips is constructed as described in Section 6.6. This enables the excitation of some internal modes for specific heights of the curly strips according to the operating frequency of the PolSAR. For such a model, the dependence of the Gaussian weighted average RVI on the grass height is presented in Figure 17 for a PolSAR operating at a frequency 1.27 GHz with look angle $\theta_i = 40°$. The RVI for the grassland model B is clearly affected by the internal resonances. As shown in this figure, the RVI for grassland model B has sharp peaks at some discrete heights of the grass corresponding to internal resonances of specific orders. In comparison with the RVI for the grassland model A, which is the reference curve to estimate the grass height, the RVI of the grassland model B shows considerable differences. Consequently, this leads to considerable errors in the estimated grass height.
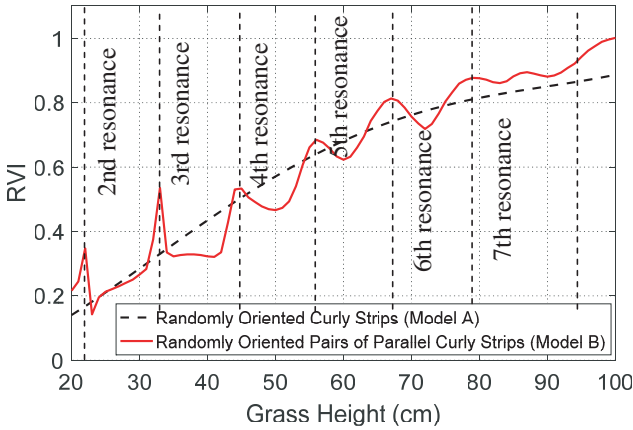

Figure 17. The Gaussian weighted average of the RVI against grass height at the presence of the internal resonances at 1.27 GHz.
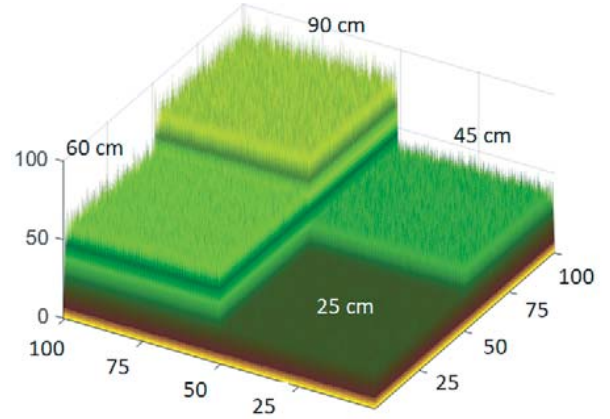

Figure 18. Inhomogeneous grassland area composed of four quarters of different homogenous grass heights using clouds of random curly strip-wires.

Figure 18 shows a geometrical model for an inhomogeneous square grassland area ($100\,\text{m} \times 100\,\text{m}$) composed of four quarters of different average grass heights ($25, 45, 65, 90\,\text{cm}$). This model is constructed using clouds of curly strips as described in Section 4. For the sake of evaluating the RVI as measured by PolSAR system, a four-channel PolSAR image with resolution of $1\,\text{m} \times 1\,\text{m}$ is constructed for this grassland area through EM simulation. To get the generated grassland area free from internal modes, the grassland model A is used to generate a $1\,\text{m} \times 1\,\text{m}$ grassland cell of homogeneous height distribution corresponding to each pixel of the image so as to construct the entire inhomogeneous grassland area.

To demonstrate the effect of the internal resonances on the accuracy of the retrieved grass height by applying the method described in Section 6.3, the same geometric model for inhomogeneous grassland area as that considered in the previous case is constructed using grassland model B instead of model A. The pairs of axially-parallel curly strips found in model B enable the excitation of the internal resonances according the SAR operating frequency. For both areas of inhomogeneous grasslands, the image of the RVI obtained from the simulated PolSAR image through EM simulation is presented in Figures 19(a) and (b) for the grassland composed of cells of model A and that composed of model B, respectively. The RVI values are indicated using a color code specially made to appropriately display the RVI as an indicator for the vegetation density. By comparison between Figures 19(a) and 19(b), it is shown that the RVI is significantly affected by the excitation of the internal modes within the grassland constructed using cells of model B.

It is required to retrieve the grass heights at the positions corresponding to the pixels of the RVI image. This can be achieved by applying the method described in Section 6.3 through the fitted
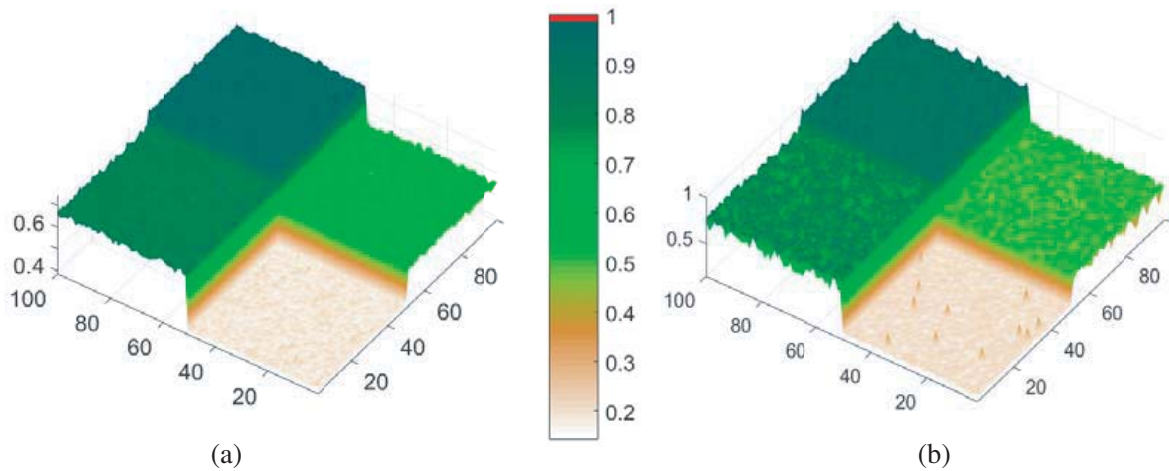
Figure 19. RVI images obtained by EM simulation of land imaging PolSAR. (a) Model A. (b) Model B.
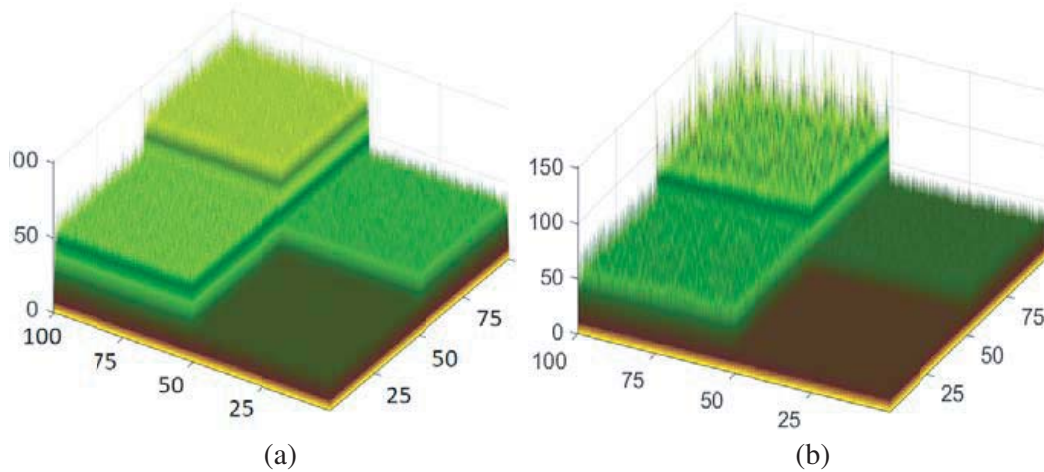

Figure 20. Recovered grassland heights using the method described in Section 6.3. (a) Model A. (b) Model B.

polynomial given by Eq. (10) or the reference curve presented in Figure 11. The retrieved grass heights are presented in Figures 20(a) and 20(b) for the grassland areas composed of cells of model A and that composed of cells of model B, respectively. A comparison between the heights of the original grassland area presented in Figure 18 and the estimated heights presented in Figure 20(a) shows almost identical heights at all the positions within the grassland area. On the other hand, the retrieved heights for the grassland area composed of cells of model B show significant deviations compared with the original grassland heights shown in Figure 18.

The errors of retrieved grass heights for all the pixels of the image are presented in Figures 21(a) and 21(b) for the grassland areas composed of cells of model A and that composed of cells of model B, respectively. It is clear that the errors are very low and are negligible for the grassland of model A compared to the errors arising due to the internal resonances for the grassland of model B. The percentage error in the retrieved grass height averaged over the image pixels is about 0.45% for the grass land of model A. Such a low percentage error in the estimated grass height in the absence of the internal modes reflects the efficiency of the proposed method to estimate the grass height using the RVI measured by PolSAR system. On the other hand, the averaged percentage error is about 11.5% for the grassland of model B. The maximum error in the grass height estimation is that encountered for the grassland quarter of 90 cm height (at many pixels within the image area corresponding to this quarter).
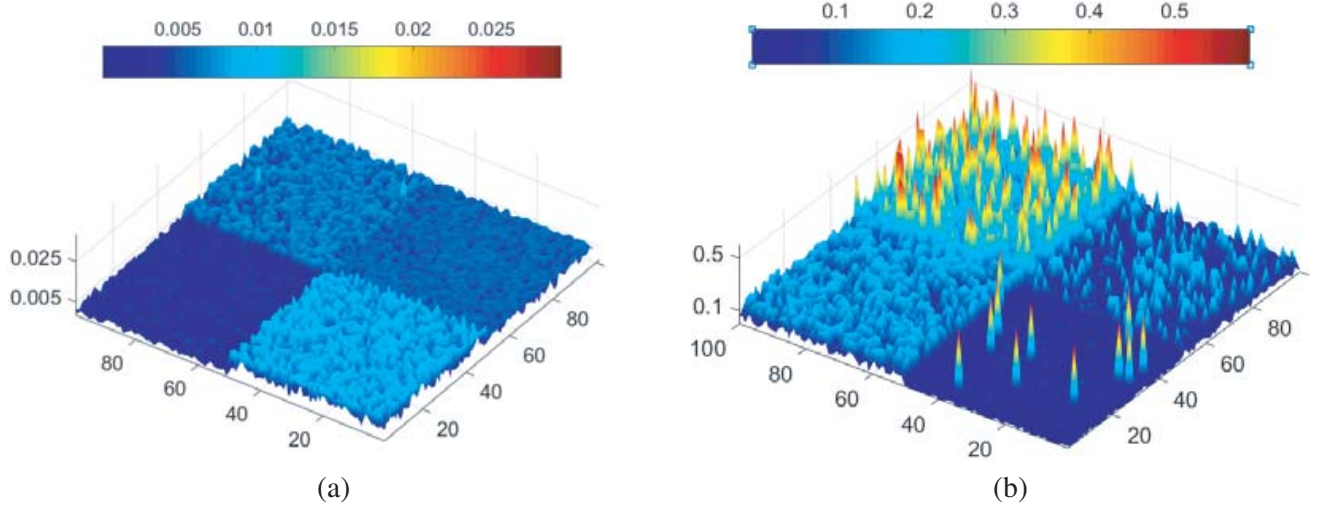
(a)   (b)

Figure 21. The relative errors in the recovered grass heights for (a) grassland area without internal modes and (b) grassland area affected by internal modes. (a) Model A. (b) Model B.

This can be explained in view of the curve representing the dependence of the RVI on the grass height shown in Figure 17. It is clear that large differences between the RVI obtained for grassland free from internal resonances and that obtained for grassland with excited internal resonances occur around a grass height of 90 cm. Also, for the land quarter with a grass height of 25 cm, significant error in the estimated height occur at a few separate pixels within the image area corresponding to this quarter. This can be attributed to that the grass cloud of such a height is close to the conditions required to excite the 2nd-order internal resonance at the operating frequency of the PolSAR system (1.27 GHz).

In conclusion, one can say that the average error in the estimated grass height for the grassland model including pairs of axially-parallel curly strips may be considerably higher than the error encountered for the grassland model free from parallel pairs.

It may be worthwhile to mention that the aim of the present paper has been to introduce the main idea of the method proposed for grassland height retrieval using the RVI (as conventionally defined). The proposed method is introduced under the assumption of optimal environmental and operational conditions during the land-imaging process. Besides, some models of the grasslands have been constructed for quantitative assessment of the proposed method through the numerical results of electromagnetic simulation. For sure, the electromagnetic propagation impairments, such as ionosphere, rain, cloudy atmosphere [18, 19], and strong winds, can have significantly bad effects on the proposed method. Moreover, the SAR receiver noise and interfering signals can also affect the accuracy of the grass height retrieval. Of course, the assessment of such negative effects needs a great deal of research effort especially those causing depolarization of the electromagnetic scattering that may lead to erroneous RVI data. However, good treatment of the consequences of such negative effects is affordable as the RVI data itself (as collected by PolSAR systems) has been proved to be amenable to such bad environmental conditions, and hence, there is still a great chance for efficient application of the proposed method. Moreover, the expression of the RVI itself can be modified [20] to get more realistic representation for the volume scattering due to vegetation only and to minimize the clutter effects.

7. CONCLUSION

A method for monitoring the natural grass height through PolSAR data is proposed. In the natural grass land consisting of long narrow leaves, it frequently happens to find equal and axially-parallel leaves resulting in a microwave cavity or internally resonant modes. These modes are studied, and their effects on the estimation of the grass height are investigated. For the evaluation of the backscattering coefficients S_{hh}, S_{vh}, S_{hv}, and S_{vv} through EM simulation, a grassland area is modelled as a cloud of highly conductive random curly strips. A new method is proposed to use the RVI for the purpose of

measuring the grass height. It is shown that singular sharp peaks of the RVI-frequency curve due to the excitation of internally resonant modes may lead to erroneous recovery of the grass height. The percentage error of the estimated grass height when some internal modes are excited is found to be higher than the error encountered for the grassland model free from such internal resonances.

REFERENCES

1. Huang, Y., J. P. Walker, Y. Gao, X. Wu, and A. Monerris, "Estimation of vegetation water content from the radar vegetation index at L-band," *IEEE Transactions on Geoscience and Remote Sensing*, Vol. 54, No. 2, 981–989, 2016.

2. Ulaby, F. T. and T. F. Bush, "Monitoring wheat growth with radar," *Photogramm. Eng. Remote Sens.*, Vol. 42, No. 4, 557–568, Apr. 1976.

3. Ulaby, F. T., C. T. Allen, G. Eger, and E. T. Kanemasu, "Relating the microwave backscattering coefficient to leaf area index," *Remote Sens. Environ.*, Vol. 14, Nos. 1–3, 113–133, Jan. 1984.

4. Oh, Y. S., S. Y. Hong, Y. J. Kim, J. Y. Hong, and Y. H. Kim, "Polarimetric backscattering coefficients of flooded rice fields at L- and C-bands: Measurements, modeling, and data analysis," *IEEE Transactions on Geoscience and Remote Sensing*, Vol. 47, No. 8, 2714–2721, Aug. 2009.

5. Kim, Y. and J. Zyl, "On the relationship between polarimetric parameters," *IGARSS 2000, IEEE 2000 International Geoscience and Remote Sensing Symposium, Taking the Pulse of the Planet: The Role of Remote Sensing in Managing the Environment, Proceedings (Cat. No. 00CH37120)*, Vol. 3, 1298–1300, IEEE, 2000.

6. Haldar, D., D. Viral, M. Arundhati, and B. Bimal, "Radar vegetation index for assessing cotton crop condition using RISAT-1 data," *Geocarto International*, 1–12, 2018.

7. Szigarski, C., T. Jagdhuber, M. Baur, C. Thiel, M. Parrens, J. P. Wigneron, M. Piles, and D. Entekhabi, "Analysis of the radar vegetation index and potential improvements," *Remote Sensing*, Vol. 10, No. 11, 1776, 2018.

8. Kim, Y. and J. Zyl, "Comparison of forest estimation techniques using SAR data," *Proc. IEEE IGARSS Conf.*, 1395–1397, 2001.

9. Kim, Y., T. Jackson, R. Bindlish, H. Lee, and S. Hong, "Radar vegetation index for estimating the vegetation water content of rice and soybean," *IEEE Geoscience and Remote Sensing Letters*, Vol. 9, No. 4, 564–568, Jul. 2012.

10. Kim, Y., T. Jackson, R. Bindlish, S. Hong, G. Jung, and K. Lee, "Retrieval of wheat growth parameters with radar vegetation indices," *IEEE Geoscience and Remote Sensing Letters*, Vol. 11, No. 4, 808–812, 2014.

11. Zhang, L., Z. Bin, C. Hongjun, and Z. Ye, "Multiple-component scattering model for polarimetric SAR image decomposition," *IEEE Geoscience and Remote Sensing Letters*, Vol. 5, No. 4, 603–607, 2008.

12. Yoshio, Y., T. Moriyama, M. Ishido, and H. Yamada, "Four-component scattering model for polarimetric SAR image decomposition," *IEEE Transactions on Geoscience and Remote Sensing*, Vol. 43, No. 8, 1699–1706, 2005.

13. Freeman, A. and S. L. Durden, "A three-component scattering model for polarimetric SAR data," *IEEE Transactions on Geoscience and Remote Sensing*, Vol. 36, No. 3, 963–973, 1998.

14. Hussein, K. F. A., "Effect of internal resonance on the radar cross section and shield effectiveness of open spherical enclosures," *Progress In Electromagnetics Research*, Vol. 70, 225–246, 2007.

15. Colak, D., A. Altintas, and A. I. Nosich, "RCS study of cylindrical cavity-backed apertures with outer or inner material coating: The case of *E*-polarization," *IEEE Trans. Antennas Propagat.*, Vol. 41, No. 11, 1551–1559, Nov. 1993.

16. Soliman, S. A. M., A. E. Farahat, K. F. A. Hussein, and A. Ammar, "Spatial domain generation of random surface using savitzky-golay filter for simulation of electromagnetic polarimetric systems," *Aces Journal*, Vol. 34, No. 1, 148–161, Jan. 2019.

17. Hussein, K. F. A., "Fast computational algorithm for EFIE applied to arbitrarily-shaped conducting surfaces," *Progress In Electromagnetics Research*, Vol. 68, 339–357, 2007.

18. Kocifaj, M., V. Gorden, and K. Jozef, "Backscatter in a cloudy atmosphere as a lightning-threat indicator," *Journal of Quantitative Spectroscopy and Radiative Transfer*, Vol. 150, 175–180, 2015.

19. Kocifaj, M., K. Jozef, K. František, and V. Gorden, "Charge-induced electromagnetic resonances in nanoparticles," *Annalen der Physik*, Vol. 527, Nos. 11–12, 765–769, 2015.

20. Szigarski, C., T. Jagdhuber, M. Baur, C. Thiel, M. Parrens, J. P. Wigneron, M. Piles, and D. Entekhabi, "Analysis of the radar vegetation index and potential improvements," *Remote Sensing*, Vol. 10, No. 11, 1776, 2018.